INTERNATIONAL JOURNAL OF
RECENT TRENDS IN MULTIDISCIPLINARY RESEARCH
Special Issue, March-April 2023, Vol 3 (02), 31-38.
International conference on Innovation towards Sustainable Development Goals-ICISDG'23 ISSN No: 2583 0368

A Wide Conversion Ratio Bidirectional Modified SEPIC Converter with Non dissipative Current Snubber

R.Selciya[1], V.K.Rakesh[2], E.A.Harini[3], L.Chitra[4]
[1, 2, 3] *Electrical and Electronics Engineering, Dr. Mahalingam College of Engineering and Technology, India.*
[4] *Associate Professor, Electrical and Electronics Engineering, Dr. Mahalingam College of Engineering and Technology, India.*

Article Type: Research

OPENACCESS
Article Citation:
R.Selciya[1], V.K.Rakesh[2], E.A.Harini[3], L.Chitra[4], "A Wide Conversion Ratio Bidirectional Modified SEPIC Converter With Non dissipative Current Snubber", International Journal of Recent Trends In Multidisciplinary Research, March-April 2023, Vol 3(02), 31-38.

https://www.doi.org/10.59256/ijrtmr.20230402c08

Abstract: This article presents a wide conversion ratio bidirectional dc-dc converter based on a bidirectional modified Single-ended primary-inductor converter (SEPIC converter). A key feature of this modified SEPIC converter is the non-dissipative current snubber circuit, which is used to achieve zero current switching and to suppress voltage spikes that occur during MOSFET switching. The snubber is made up of a capacitor, an inductor, and a diode that work together to form a resonant circuit that absorbs the voltage spike and returns it to the circuit without dissipating it. Even with conventional MOSFETs, high efficiency is achieved. The SEPIC converter differs from other bi-directional DC-DC converters in that it provides continuous output current, has fewer components, and can provide high conversion ratios of step-up and step-down voltage without exceedingly low or high duty-cycle. This paper presents a theoretical analysis with stages of operation in both step-up and step-down modes, theoretical waveforms, and the design procedure, as well as a comparison with other bidirectional dc-dc converter topologies. The experimental results are presented to validate the performance of the proposed converter using a 500-W prototype with Voltage Source V_1 = 48 V and Voltage SourceV_2 = 300 V.
Key Word: DC-DC Converters; Current Snubber; Power Electronics.

1. Introduction

Applications for energy storage systems include renewable energy systems, micro grids, electric cars, uninterruptible power sources, and mobile electronic devices. The storage component is a buffer that stores extra energy, releases it when needed, and makes compensation for the power imbalance between power generation and consumption. In systems like these, the storage components for energy are connected to the rest of the system by bidirectional dc-dc power converters (BDCs), which are a key component. Super- and ultra capacitors, batteries with various technologies, and other low-voltage devices are frequently utilized as the storage element. These are generally low-voltage devices. In order to meet the voltage requirements, use of lengthy series of strings of storage elements can lead to issues such as charge imbalance, lifetime reduction, and reliability issues. As a result, the storage device's maximum dc voltage is constrained. On the other hand, some applications may also require a high dc source in comparison to the storage element's voltage; in these circumstances, a Bidirectional DC-DC Converter with a high conversion ratio is required.

When super capacitors are charged or discharged, their voltage varies across a large range, which results in wide conversion ratio. Bi-directional DC Converters are challenging when efficiency, power density, complexity, and cost are taken into account. BDCs can be developed using either an isolated or non isolated topology. By adjusting the transformer turns ratio, isolated topologies can quickly achieve large conversion ratios. Unfortunately, these architectures typically include a lot of switches, are expensive, and have a low power density. The most common non isolated BDC architecture is the traditional buck/boost topology, which has only two active switches and a simple construction. The usage of this topology is limited. There are issues such as intrinsically poor static gain and hard-switching operation. There is also extreme duty-cycle and also severe reverse recovery current of the intrinsic switch diodes.

To address these issues with the traditional buck/boost BDC, other strategies have been presented. One configuration is the addition of several techniques for increasing the traditional buck/boost topology's conversion ratio. These changes typically result in an increase in the number of switches being used and the complexity of the circuit but

allow the non isolated BDC's conversion ratio and application range to be expanded.

The technique of coupled inductor, as shown in [3]–[5], is an effective method. The conversion ratios can be increased by adjusting the ratio of inductor turns. The leakage inductance can enhance commutations and reduce problems with reverse recovery in intrinsic switches diodes. To resolve the problems with switches overvoltage caused on by inductor energy leakage, however, a significant amount of work in topology creation is required. The coupled inductor based high conversion ratio BDC is a high-performance structure that addresses the issues of inductance energy leakage while operating with lower voltage stress and also for maintaining comparatively less number of switches. The switched capacitor method used to create hybrid converters is an additional option.

They are modular structures with a high conversion ratio and low voltage stress. The construction of a topology with a less number of switches and capacitors presents a difficulty for this method. To maintain low switching losses, certain design parameters and modulation must be considered. In [6] and [7], some high-performance and high conversion ratio topologies utilizing hybrid converters are suggested. The combination of coupled inductors and switched-capacitor devices is another intriguing layout that effectively combines the benefits of both approaches. Switch overvoltage issues can be resolved by using the coupled inductor leakage energy during the operation of switched-capacitor cells. Yet creating a simple structure with less switches is difficult.

2. Materials and Methods

A. Proposed Design

There are several applications for the conventional step-up/step-down unidirectional SEPIC dc-dc converter. However, this topology has certain disadvantages, including a limited and restricted static gain and a high semiconductor voltage stress on the semiconductors that is equal to the total sum of the output voltages and input voltages. The bidirectional modified SEPIC converter shown in Fig. 1 is a unidirectional structure with a high static gain that operates with reduced semiconductor voltage stress . It was proposed in [15] and [16].

This converter has a high efficiency and has been employed in a variety of applications, including LED drivers [23], motor drive systems [24], high power factor rectifiers [15], and renewable energy systems [16] – [19]. This article introduces the usage of the architecture as a BDC, which has not yet been suggested. It describes the development of a BDC with a large conversion ratio utilising the modified SEPIC converter, which only requires three switches and has an intrinsically high static gain and low voltage stress. The improved SEPIC converter can use some high static gain techniques like coupled inductors and switched capacitors, but the basic structure operation is shown in this paper.

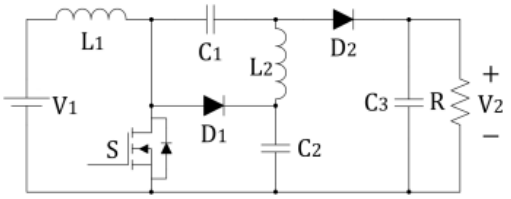

Fig. 1 Modified SEPIC Converter

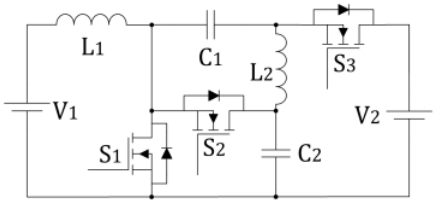

Fig. 2 Bidirectional Modified SEPIC Converter

To convert the original actual unidirectional converter shown in Figure 1 into a bidirectional structure, the diodes D1 and D2 must first be changed to the active switches S_2 and S_3, as illustrated in Figure 2. The switches S2-S3 are controlled simultaneously and complementary to S_1 switch. The proposed DC-DC converter with current snubber circuit for obtaining soft switching is presented in Figure 3.

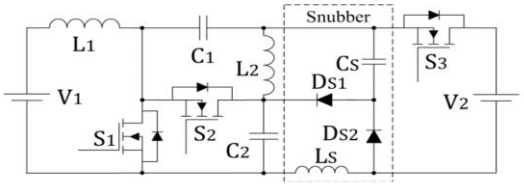

Fig. 3 Bidirectional Modified SEPIC Converter with Current Snubber

B. Operation Stages

The voltage source V_2 is assumed to be higher than the voltage source V_1, and the proposed converter presents two stages of operation such as the step-up mode and the step-down mode. The operation stages are same in the step-up and step-down mode only with the current flow inversion. The theoretical analysis of this dc-dc converter is presented in the step-up mode, and then, there are some considerations in the step-down operation and they are presented.

1) Operation Stage – FIRST —Step-Up Mode of Operation [Fig. 4(a)]: The active switch S_1 is turned ON in this stage, and the other switches S_2 and S_3 are turned OFF, and is presented in Fig. 4(a). The two inductors L_1 and L_2 are storing energy with the voltage value V_1 having applied across the inductor L_1 and the voltage $(V_{C2} - V_{C1}) = V_1$applied across the inductor L_2.

2) Operation Stage – SECOND —Step Up Mode of Operation [Fig. 4(b)]: S_1switch is turned to off condition, and the intrinsic diodes of the switches S_2 and S_3begins to conduct the inductors currents. Energy transference is seen from the inductors L_1 ,L_2 to the capacitors in this converter during this stage of operation, that is depicted in Fig. 4(b). The voltage that is applied across the inductors L_1 and L_2 is equal to $-(V_{C2}-V_1) = (V_1 - V_{C2})$ for L_1 and $-(V_2 - V_{C2}) = (V_{C2} - V_2)$ for L_2.

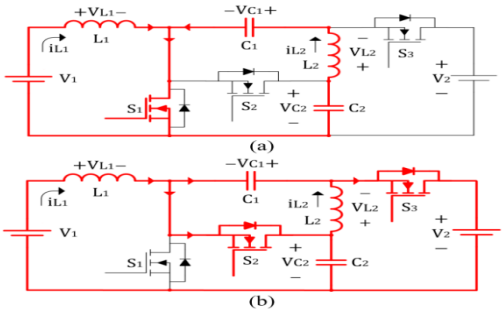

Fig. 4 Step-up modes of Operation. (a) Stage 1. (b) Stage 2.

C. Main Ideal Waveforms

The theoretical waveforms after analyzation in all the components that operating in the step-up mode of operation are shown in Fig. 5. The switches S_1-S_2-$S_3$with the voltage across them is equal to V_{C2} and is much less than the output voltage which is equal to $V_2 = (V_{C1} + V_{C2})$. The average currents of the inductor L_1 and L_2 are equal to the voltages V_1 and V_2 average currents.

D. Static Gain

At steady state, in the inductorsL_1 and L_2, the average voltage is identified to be null. This is represented in the equations below:

$$V_{L1\_avg} = V_1 \cdot D + (V_1 - V_{C2}) \cdot (1 - D) = 0 \quad (1)$$

$$V_{L2\_avg} = (V_{C2} - V_{C1}) \cdot D + (V_{C2} - V_2) \cdot (1 - D) = 0. \quad (2)$$

Using Eqn.(1), the voltage that is present across the Capacitor C_2 is obtained. It is equal to the boost converter static gain. It is shown in Eqn.(3). The voltage across all the semiconductors such as S_1,S_2,S_3 is equal to the V_{C2}(Voltage of Capacitor).

$$V_{C2} = \frac{V_1}{1 - D}. \quad (3)$$

We consider that at the steady state, the average voltage in the inductors L_1 and L_2 as null, the relation that is between the capacitors C_1 and C_2can be obtained and is equal to the following equation:

$$V_{C1} = V_{C2} - V_1. \quad (4)$$

In Eqn.(4) replacing Eqn.(3), the voltage that is present across the capacitor C_1 can be obtained and is presented in the equation below:

$$V_{C1} = \frac{V_1 \cdot D}{1 - D}. \quad (5)$$

In Eqn.(2), on replacing Eqn.(3) and Eqn.(5)the static gain of the converter is calculated and is shown in the equation below:

$$\frac{V_2}{V_1} = \frac{1 + D}{1 - D}. \quad (6)$$

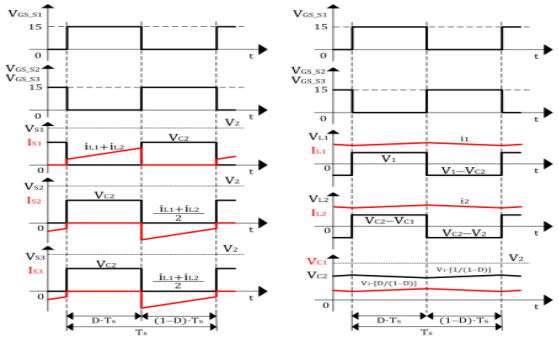

Fig. 5 Bidirectional Modified SEPIC Converter with Current Snubber Circuit

E. Inductors Design

Using the function of the ripple of the current ($\Delta i_{L1} - \Delta i_{L2}$), the inductors L_1 and L_2values can be calculated. The voltage that is applied to L_1 and L_2 during the ON stage of the switch S_1 is identified to be equal to voltage V_1, as seen in Eqn.(7) and Eqn.(8). The L_1 and L_2inductors average currents are approximately equal to the average current so V_1 and V_2 average currents.

$$L_1 = \frac{V_1 \cdot D}{\Delta_{iL1} \cdot f_s} \qquad (7)$$

$$L_2 = \frac{V_1 \cdot D}{\Delta_{iL2} \cdot f_s}. \qquad (8)$$

F. Capacitors Design

Using the specification of the voltage ripple ($\Delta V_{C1} - \Delta V_{C2}$) and through the variation of charge the values of the C_1 and C_2 capacitors are calculated. The current that is present across the capacitors C_1 and C_2 during the stage 1 of operation is observed to be equal to the current of the Inductor L_2 , and the average value is averagely equal to the average current of V_2 (i_{V2}). The capacitor C_1 and C_2values are then calculated using the equations below:

$$C_1 = \frac{i_{V_2} \cdot D}{\Delta_{VC1} \cdot f_s} \qquad (9)$$

$$C_2 = \frac{i_{V_2} \cdot D}{\Delta_{VC2} \cdot f_s}. \qquad (10)$$

G. Nondissipative Current Snubber

To the wide conversion ratio bidirectional modified Single Ended Primary Inductor Converter, a current snubber circuit that is nondissipative is proposed. It uses only passive components. It is used for the purpose of reducing the switching losses and to allow the usage of Si MOSFETs. The proposed DC-DC converter along with the inclusion of the current snubber circuit is shown in Fig. 3. The current snubber circuit consists of a one small resonant inductor L_S, one capacitor C_S, and there are two diodes that is D_{S1} and D_{S2}. By including the proposed snubber circuit with the converter the *di/dt*is constrained and also the reverse recovery current of the intrinsic switches diodes are limited. During Turn-ON, it operates with the Zero Current Switching commutation and during Turn-OFF, it operates with the Zero Current Switching commutation at some switches.

The traditional PWM modulation along with the simultaneous command of S_2 and S_3 switches and by giving the complementary command to the S_1switchhas to be changed with the proposed current snubber circuit to obtain all the operational stage advantages in both the step-up mode and step-down modes.

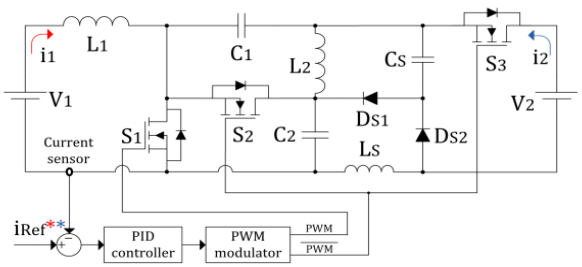

Fig. 6 Bidirectional modified SEPIC converter with current snubber and current control loop

H. Operation Stages with Current Snubber - Step Up Mode

The stages of operation of the bidirectional modified SEPIC converter that is operating in both the step-up and step-down modes with the current snubber are shown in Figs. 6 and 7, respectively, and Fig. 8 displays the theoretical waveforms. The intrinsic diodes of the S_2 and S_3switches conduct in a complimentary manner when the S_1switch is commanded. The converter operation, which comes before the switch S_1 conduction command, is the first operation stage

considered. Fig. 8 displays the command signals for the switches with the delay (α).

1) First Operating Stage [Fig. 6(a)]: By the intrinsic diode of the S_3 switch, energy is transferred from the L_1 and L_2inductors to the source V_2,the currents through L_1 and L_2 fall linearly. With providing the command for the S_1 switch to turn ON, this stage is finished.
2) Second Operating Stage[Fig. 6(b)]:When the S_1switch is turned ON, the current of the switch increase slinearly, and the S_3 switch intrinsic diode current decreases linearly, with the di/dt of each being constrained by the L_s inductor. (V_2-V_{C1}) is the voltage that is applied across the inductor L_s. With the voltage V_1 supplied to its terminals, the inductors L_1 and L_2 are storing energy. The inductor L_s imposes a di/dt limitation so that the S_3 intrinsic diode is blocked. It is blocked without reverse recovery current. This stage of operation is complete when the current across it is zero.
3) Third Operating Stage [Fig. 6(c)]: The energy accumulated in the L_S inductor during the previous stage of operation is transferred to the C_S snubber capacitor through the S_1switch when the S_3 intrinsic diode is being blocked. When the D_{S2} current diode reaches zero, this resonant energy transmission is complete.
4) Fourth Operating Stage [Fig. 6(d)]:TheL_1 and L_2 inductors continue to store energy as normally without the current snubber shown in Fig. 3 (a) since the D_{S2} diode is blocked, allowing just the S_1 conduction. During the S_1, this stage of operation is maintained.
5) Fifth Operating Stage[Fig. 6(e)]:The S3 intrinsic diode conducts while the switch S_1 is off, and the inductor L_s limits the linear increase in current through this diode. Through D_{S1}, the energy that was stored in C_s during the third operating step is discharged. When the D_{S1} current is zero and this diode is blocked, this stage is complete.
6) Sixth Operating Stage [Fig. 6(f)]: The S_2 intrinsic diode conducts when the D_{S1} diode is blocked. When the S_2switch intrinsic diode current falls linearly, it continues to increase in the S_3 intrinsic diode. The intrinsic diode of the switch S_2 is zero blocking this diode and is blocking without any reverse recovery current when the current in the L_1 inductor is equal to the L_S current. Energy is transferred from L_1 and L_2 to V_2 while the S_2 is blocked, maintaining the first stage of operation.

I. Operation Stages with Current Snubber - Step Down Mode

Fig. 7 and 8 illustrate the theoretical waveforms and the operational stages of the modified SEPIC converter working in the step-down mode of operation with a current snubber. The S_1 intrinsic switch diode conducts in a complimentary manner when the S_2 and S_3 switches are commanded. The converter operation, which comes before the switch S_1 conduction command, is the first operation stage to be considered.

1) First Operating Stage [Fig. 7(a)]:The energy stored in the L_1 inductor is transmitted to the source V_1 during this free-wheeling stage, while the energy that is stored in the L_2 inductor is then transferred via the S_1 intrinsic diode to the capacitor C_2. When the S_3 is turned ON, this stage of operation is complete.
2) Second Operating Stage [Fig. 7(b)]:Due to the delay (α) in this switch's command, the switch S_2 remains off when the switch S_3 is turned on with ZCS. While the current in the S_1 intrinsic diode falls linearly and is constrained by the inductor L_s, the S_3 current increases linearly. Inductors L_1 and L_2 current increases linearly. This stage is complete when the current of the S_1intrinsic diode drops to zero, blocking the diode without reverse recovery current due to the inductor L_s's limitation on the diode/dt ratio.
3) Third Operating Stage [Fig. 7(c)]:The diode D_{S1}starts conducting when the intrinsic diodeof S_1switch is blocked. The C_s and C_2capacitors are then charged and transfers energy from the voltage source V_2 via snubber diode D_{S1} and the snubber inductor L_s. The $L_s$snubber inductor current and S_3 current falls linearly. During this stage, the switch S_2 can be turned ON.
4) Fourth Operating Stage [Fig. 7(d)]:With ZCS, the S_2switch is activated, and there is a linear increase of current. By charging the snubber capacitor C_S till the D_{S1} current is zero, this diode is blocked without any current of reverse recovery.
5) Fifth Operating Stage [Fig. 7(e)]:The D_{S1} diode being blocked indicates the start of this step. The S_3 current drops at the same proportion as the S_2 current, which continues to increase linearly. The L_S current (Snubber inductor current) and the switch S_3 current are both zero at this point.
6) Sixth Operating Stage [Fig. 7(f)]: At this phase, the switch S_2 transfers energy to the source V_1 by conducting the currents of the inductors L_1 and L_2.Throughout the energy transfer, the S_2switch current and the inductors' currents continue to increase linearly. During the simultaneous switching OFF of the switches S_2 and S_3, this stage is complete.
7) Seventh Operating Stage[Fig. 7(g)]:The S_1 intrinsic diode conducts when the switches S_2 and S_3 are off, triggering the start of the L_1 and L_2 inductor currents' free-wheeling stage. Moreover, there is the resonant energy transfer fromC_s to C_1 via diode D_{S2} and L_s. Upon completion of this cycle of resonance, the diode D_{S2} is blocked, and thus returning back to the initial operating stage.

J. Design of Snubber

Using the minimum time delay (α) specification that has to be more than the interval Δt_2that is shown in the analyzed theoretical waveforms at the step-down mode of operation that is represented in Fig. 8(b),the value of the Ls inductor can be calculated. Hence, the calculation is presented in the equations below (Eqn 11 and 12):

$$\alpha = \frac{L_S \cdot (I_{L1} + I_{L2})}{V_1 + V_{C2}}. \qquad (11)$$

$$L_S = \frac{a \cdot (V_1 + V_{C2})}{(I_{L1} + I_{L2})}. \qquad (12)$$

The snubber capacitor value C_S can be calculated using the specification of the inductor L_s by using the definition of the period of resonant (To) of the transference of resonant energy. The calculation is done using the below formula. :

$$\frac{T_o}{2} = \pi \cdot \sqrt{L_S \cdot C_S}. \qquad (13)$$

Eqn. (14) represents the maximum voltage that is across the snubber circuit diodes. In the theoretical waveforms, it is observed that the snubber diodes conduction period is reduced. In these diodes, the average current is low. The specification of the snubber diodes is seen as a function of the peak circuit current

$$V_{DS1} = V_{DS2} = V_{C2} = \frac{V_1}{1 - D}. \qquad (14)$$

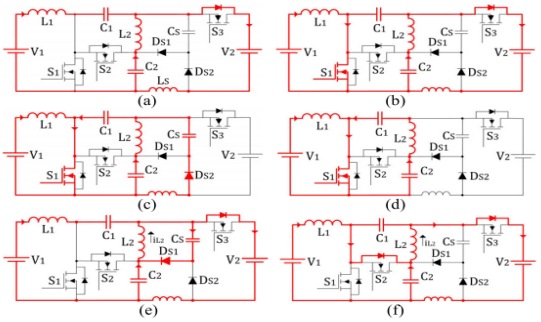

Fig. 6. Stages of Step-up mode of operation with the current snubber.

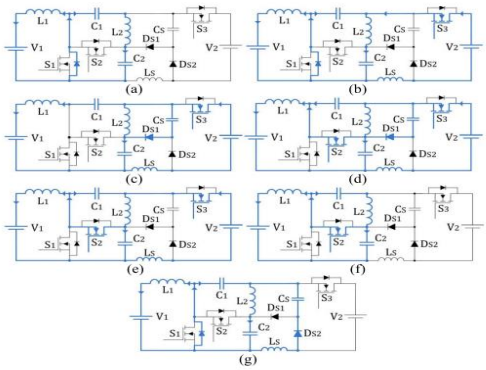

Fig.7. Stages of Step-down mode of operation with current snubber

3. Results and Discussion

A. Result

The mode of operation is considered to be step-up when there is a flow of current from the voltage source V_1 to V_2, and the mode of operation is considered to be step-down when there is a flow of current from the voltage source V_2 to V_1.The waveforms of both voltage and current of S_2switch isseen in Fig. 8. In the step-down mode of operation,the turn ON is Zero Current Switching. In the step up mode of operation, Zero Current Swtichin and the soft switching is offered by this switch.The maximum voltages obtained at S_2 was 196 V and 212 V at step-up mode of operation and step-down mode of operation respectively. The average current obtained at S_2 was 2.56 A and 4.98 A at step-up mode of operation and step-down mode of operation respectively.

Fig. 9 shows the waveforms of voltage that is across theC_1 and C_2 capacitors. The capacitorsC_1 and C_2 have voltages values that are equal to the traditional buck-boost and boost converters output voltages, respectively. The switches are operating atV_{C2}which is their maximum voltage, it is smaller than the value of voltage V_2. A 10% voltage ripple specified in the design was actually observed.

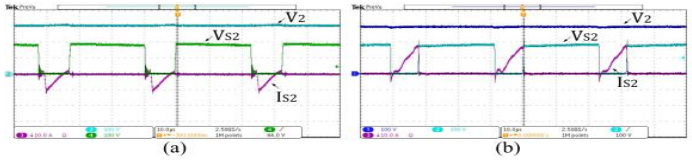

Fig.8.Voltage and Current of Switch S_2.
a) Step-up mode(b) Step-down mode.

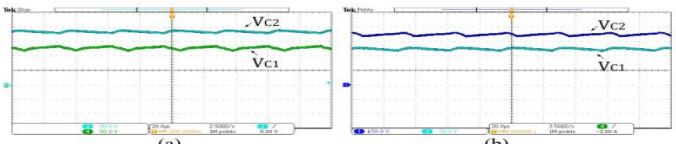

Fig.9.Capacitors voltages C_1–C_2 (a) Step-up mode. (b) Step-down mode.

While Fig. 10(b) depicts the transient from the step-down mode to the step-up mode, Fig. 10(a) depicts the current flowing through inductor L_1 during the transition from the step-up mode to the step-down mode. The converter can function with a bidirectional power flow, according to the results. According to the block diagram, the closed-loop operation is implemented through current control in the low-voltage side of the converter. It is depicted in Fig.3. To obtain proper transient response and zero steady-state error, a PID controller configuration was realized. In the control reference positive and negative steps of 5 A are applied.

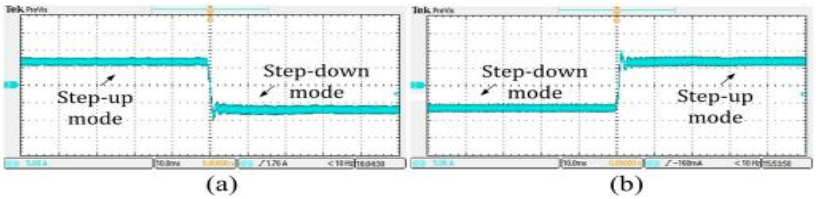

Fig.10 Inductor L1 current operating with the closed current control loop.
(a) Step-up to step-down transient. (b) Step-down to step-up transient.

The efficiency curves for both modes of operation as a function as a function of the output power for the switching frequency equal to 30kHz is calculated. The converter's efficiency peaked at 95.9% and 96.1% for the step-up and step-down modes, respectively, while processing half of its rated power. For step-up and step-down modes, respectively, the observed efficiencies are 95.2% and 95.6% at rated power.

The proposed converter is based on a bidirectional modified SEPIC converter operates with three active power switches with lower switching losses and also less voltage stress. With fewer switches used than in other topologies, a high level of efficiency was achieved.

B. Discussion

Table IV compares the proposed converter with more recent wide conversion ratio bidirectional converters (2018-2019) that have comparable specs and employ four distinct principles. The switching capacitor is used in converter 1 in [7]. It operates with a high conversion ratio and a smaller voltage stress on switches. Switching losses are minimized and have the least number of passive components. The achieved efficiency is close to 90% and uses four switches. The quasi-Z-source structure is used by the converter 2 shown in [14] to function with a high conversion ratio.

Table I Converter Comparison

Converter	1 [7]	2 [14]	3 [11]	4 [3]	5 [1]	Proposed
Principle of Operation	Switched Capacitor	Quasi-Z-Source	Resonant	Coupled Inductor		Modified SEPIC
Switching Losses	Low	Moderate	Low	Low	Low	Low
Efficiency Step-up Step-down	90.08% 90.86%	88.17% 92.31%	95.50% 95.00%	94.50% 94.00%	94.7% 93.00%	95.20% 95.60%
Specifications	P = 300 W V1 = 40 V V2=300V 20kHz	P=300W V1 = 40V V2 = 240V 20kHz	P=350W V1 = 48V V2 =380V 105kHz	P=500W V1 = 40V V2 =400V 50kHz	P=250W V1 =36 VV2 =84V100k Hz	P=500W V1 = 48 V V2 = 300V 30kHz
Conversion Ratio	7.5	6.0	7.9	10	6.15	6.25
Number of Switches	4	3	4	4	3	3
Voltage Stress on Switches	S_1-$S_2$0.5.V_2 S_3–$S_4$0.5.V_2	S_1-$S_2$0.57.V_2 $S_3$0.57.V_2	S_1- $S_2$0.5.V_2S_3 –$S_4$1.0.V_2	S_1- $S_2$0.2.V_2S_3– $S_4$0.8.V_2	S_1- $S_2$0.2.V_2S_3– $S_4$0.8.V_2	S_1- $S_2$0.57. $V_2S_3$0. 57.V_2
Power Circuit Inductors	1	2	3	2	3	2
Snubber Diodes Capacitor Inductor	- - -	- - -	- - -	- - -	- - -	2 1 1
Power Circuit Capacitor	2	2	5	2	2	2

Of the topologies that were compared, this topology has the fewest switches and the simplest circuit. The efficiency when using the step-up mode is the lowest compared to the other topologies and the switching losses are larger. The most efficient of the evaluated topologies is Converter 3, which employs a resonant arrangement and soft switching. Comparing the previous topologies, Converter 3 has the most components and employs four switches.

C. Conclusion

This article presents a bidirectional modified SEPIC DC-DC converter with a high conversion ratio. The bidirectional modified SEPIC Converter allows the usage of the semiconductor switches with much lower conduction losses by reducing the voltage stress that is present across the power switches. The non dissipative current snubber circuit that is included in the converter contributes to the power switches' soft commutation. As there was the problem of reverse recovery of their intrinsic diodes of the switches, the introduction of the current snubber circuit eliminates it.

References

[1]. *J. De Matos, F. E Silva, and L. Ribeiro, "Power control in AC isolated microgrids with renewable energy sources and energy storage systems," IEEE Trans. Ind. Electron., vol. 62, no. 6, pp. 3490–3498, Jun. 2015, doi: 10.1109/tie.2014.2367463.*

[2]. *L.-S. Yang and T.-J. Liang, "Analysis and implementation of a novel bidirectional DC–DC converter," IEEE Trans. Ind. Electron., vol. 59, no. 1, pp. 422–434, Jan. 2012, doi: 10.1109/TIE.2011.2134060.*

[3]. *M. P. Shreelakshmi, M. Das, and V. Agarwal, "Design and development of a novel high voltage gain, high-efficiency bidirectional DC–DC converter for storage interface," IEEE Trans. Ind. Electron., vol. 66, no. 6, pp. 4490–4501, Jun. 2019, doi: 10.1109/tie.2018.2860539.*

[4]. *R.-J. Wai, R.-Y. Duan, and K.-H. Jheng, "High-efficiency bidirectional dc–dc converter with high-voltage gain," IET Power Electron., vol. 5, no. 2, pp. 173–184, 2012, doi: 10.1049/IET-PEL.2011.0194.*

[5]. *Y. T. Yau, W. Z. Jiang, and K. I. Hwu, "Bidirectional operation of high step-down converter," IEEE Trans. Power Electron., vol. 30, no. 12, pp. 6829–6844, Dec. 2015, doi: 10.1109/TPEL.2015.2392376.*

[6]. *A. A. Fardoun, E. H. Ismail, A. J. Sabzali, and M. A. Al-Saffar, "Bidirectional converter with low input/output current ripple for renewable energy applications," in Proc. IEEE Energy Convers. Congr. Expo., Sep. 2011, doi: 10.1109/ecce.2011.6064217.*

[7]. *Y. Zhang, Y. Gao, L. Zhou, and M. Sumner, "A switched-capacitor bidirectional DC–DC converter with wide voltage gain range for electric vehicles with hybrid energy sources," IEEE Trans. Power Electron., vol. 33, no. 11, pp. 9459–9469, Nov. 2018, doi: 10.1109/ TPEL.2017.2788436.*

[8]. *H. Wu, K. Sun, L. Chen, L. Zhu, and Y. Xing, "High step-up/step-down soft-switching bidirectional DC–DC converter with coupled-inductor and voltage matching control for energy storage systems," IEEE Trans. Ind. Electron., vol. 63, no. 5, pp. 2892–2903, May 2016, doi: 10. 1109/TIE.2016.2517063.*

[9]. *N. Molavi, E. Adib, and H. Farzanehfard, "Soft-switching bidirectional DC–DC converter with high voltage conversion ratio," IET Power Electron., vol. 11, no. 1, pp. 33–42, Jan. 2018, doi: 10.1049/ietpel.2016.0771.*

[10]. *M. Kwon, S. Oh, and S. Choi, "High gain soft-switching bidirectional DC–DC converter for eco-friendly vehicles," IEEE Trans. Power Electron., vol. 29, no. 4, pp. 1659–1666, Apr. 2014, doi: 10.1109/ tpel.2013.2271328.*

[11]. *D. R. Patil, A. K. Rathore, and D. Srinivasan, "Non-isolated bidirectional soft-switching current-fed LCL resonant DC/DC converter to interface energy storage in DC microgrid," IEEE Trans. Ind. Appl., vol. 52, no. 2, pp. 1711–1722, Mar./Apr. 2016, doi: 10.1109/TIA.2015.2498127.*

[12]. *C.-M. Lai, Y.-C. Lin, and D. Lee, "Study and implementation of a twophase interleaved bidirectional DC/DC converter for vehicle and DCmicrogrid systems," Energies, vol. 8, no. 9, pp. 9969–9991, Sep. 2015, doi: 10.3390/en8099969.*

[13]. *H. Ardi, A. Ajami, F. Kardan, and S. N. Avilagh, "Analysis and implementation of a nonisolated bidirectional DC–DC converter with high voltage gain," IEEE Trans. Ind. Electron., vol. 63, no. 8, pp. 4878–4888, Aug. 2016, doi: 10.1109/TIE.2016.2552139.*

[14]. *Y. Zhang, Q. Liu, J. Li, and M. Sumner, "A common ground switchedquasi-Z-source bidirectional DC–DC converter with wide-voltage-gain range for EVs with hybrid energy sources," IEEE Trans. Ind. Electron., vol. 65, no. 6, pp. 5188–5200, Jun. 2018, doi: 10.1109/tie.2017.2756603.*

[15]. *P. De Melo, R. Gules, E. Romaneli, and R. Annunziato, "A modified SEPIC converter for high-power-factor rectifier and universal input voltage applications," IEEE Trans. Power Electron., vol. 25, no. 2, pp. 310–321, Feb. 2010, doi: 10.1109/tpel.2009.2027323.*

[16]. *R. Gules, W. M. Dos Santos, F. A. Dos Reis, E. F. R. Romaneli, and A. A. Badin, "A modified SEPIC converter with high static gain for renewable applications," IEEE Trans. Power Electron., vol. 29, no. 11, pp. 5860–5871, Nov. 2014, doi: 10.1109/tpel.2013.2296053.*

[17]. *R. Moradpour, A. Tavakoli, and H. Ardi, "Design and implementation of a new SEPIC-based high step-up DC/DC converter for renewable energy applications," IEEE Trans. Ind. Electron., vol. 65, no. 2, pp. 1290–1297, Feb. 2018, doi: 10.1109/TIE.2017.2733421.*

[18]. *S. Hasanpour, A. Baghramian, and H. Mojallali, "A modified SEPIC based high step-up DC–DC converter with quasi-resonant operation for renewable energy applications," IEEE Trans. Ind. Electron., vol. 66, no. 5, pp. 3539–3549, May 2019, doi: 10.1109/tie.2018.2851952*